

Shifted Chunk Transformer for Spatio-Temporal Representational Learning

Xuefan Zha, Wentao Zhu, Tingxun Lv, Sen Yang, Ji Liu
Kuaishou Technology

August 30, 2021

Abstract

Spatio-temporal representational learning has been widely adopted in various fields such as action recognition, video object segmentation, and action anticipation. Previous spatio-temporal representational learning approaches primarily employ ConvNets or sequential models, *e.g.*, LSTM, to learn the *intra-frame* and *inter-frame* features. Recently, Transformer models have successfully dominated the study of natural language processing (NLP), image classification, etc. However, the pure-Transformer based spatio-temporal learning can be prohibitively costly on memory and computation to extract *fine-grained* features from a tiny patch. To tackle the training difficulty and enhance the spatio-temporal learning, we construct a *shifted chunk Transformer* with pure self-attention blocks. Leveraging the recent efficient Transformer design in NLP, this shifted chunk Transformer can learn hierarchical spatio-temporal features from a local tiny patch to a global video clip. Our shifted self-attention can also effectively model complicated *inter-frame* variances. Furthermore, we build a clip encoder based on Transformer to model long-term temporal dependencies. We conduct thorough ablation studies to validate each component and hyper-parameters in our shifted chunk Transformer, and it outperforms previous state-of-the-art approaches on Kinetics-400, Kinetics-600, UCF101, and HMDB51. Code and trained models will be released.

1 Introduction

Spatio-temporal representational learning tries to model complicated *intra-frame* and *inter-frame* relationships, and it is critical to various tasks such as action recognition [18], action detection [50], object tracking [21], and action anticipation [19]. Deep learning based spatio-temporal representation learning approaches have been largely explored since the success of AlexNet on image classification [22, 10]. Previous deep spatio-temporal learning can be mainly divided into two aspects: deep ConvNets based methods [33, 14, 15] and deep sequential learning based methods [26, 27]. Deep ConvNets based methods are primarily integrated various factorization techniques [49, 32], or *a priori* [15] for efficient spatio-temporal learning [14]. Some works focus on extracting effective spatio-temporal features [39, 7] or capturing complicated long-range dependencies [47]. Deep sequential learning based methods try to formulate the spatial and temporal relationships through advanced deep sequential models [26] or the attention mechanism [27].

On the other hand, the Transformer has become the *de-facto* standard for sequential learning tasks such as natural language processing [42, 11]. The great success of Transformer on natural language processing (NLP) has inspired computer vision community to explore self-attention structures for several vision tasks, *e.g.*, image classification [12, 38, 34], object detection [5], and super-resolution [31]. The main difficulty in pure-Transformer models for vision is that Transformers lack the inductive biases of convolutions, such as translation equivariance, and they require more data [12] or stronger regularisation [38] in the training. It is only very recently that, vision Transform (ViT), a pure

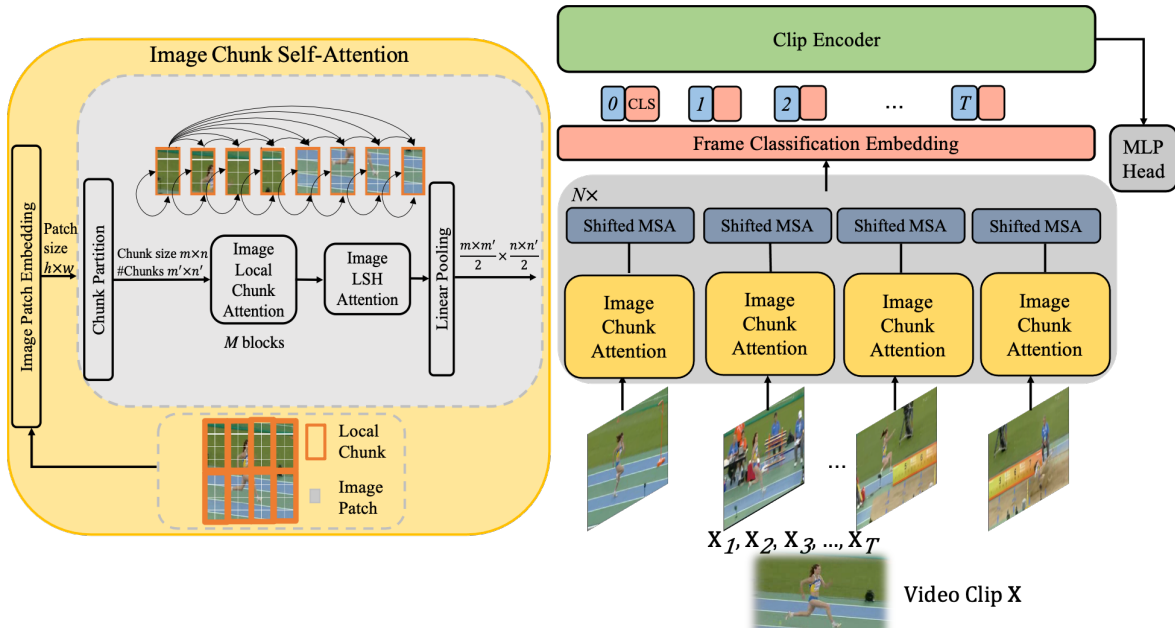


Figure 1: The framework of the proposed shifted chunk Transformer which involves two main components, frame encoder (dark grey) and clip encoder. The frame encoder consists of N alternative blocks of image chunk self-attention (left) and shifted multi-head self-attention (MSA).

Transformer architecture, has outperformed its convolutional counterparts in image classification when pre-trained on large amounts of data [12]. However, the hurdle is aggravated when the pure-Transformer design is applied to spatio-temporal representational learning.

Recently, a few attempts have been made to design pure-Transformer structures for spatio-temporal representation learning [3, 4, 13, 1]. Simply applying Transformer to 3D video domain is computationally intensive [3]. The Transformer based spatio-temporal learning methods primarily focus on designing efficient variants by factorization along spatial- and temporal-dimensions [3, 4], or employing a multi-scale pyramid structure for a trade-off between the resolution and channel capacity while reducing the memory and computational cost [13]. The spatio-temporal learning capacity can be further improved by extracting more effective fine-grained features through advanced and efficient *intra-frame* and *inter-frame* representational learning.

In this work, we propose a novel spatio-temporal learning framework based on pure-Transformer, called shifted chunk Transformer as illustrated in Fig. 1, which extracts effective fine-grained *intra-frame* features with a low computational complexity leveraging the recent advance of Transformer in NLP [20]. Specially, we divide each frame into several local windows called image chunks, and construct a hierarchical image chunk Transformer, which employs locality-sensitive hashing (LSH) to enhance the dot-product attention in each chunk and reduces the memory and computation consumption significantly. To fully consider the motion effect of object, we design a robust self-attention module, shifted self-attention, which explicitly extracts correlations from nearby frames. We further design a pure-Transformer based frame-wise attention module, clip encoder, to model the complicated *inter-frame* relationships with a minimal extra computational cost.

Our contributions can be summarized as follows:

- We construct an image chunk self-attention to mine fine-grained *intra-frame* features leveraging the recent advance of Transformer. The hierarchical image chunk Transformer employs locality-sensitive hashing (LSH) [2] to reduce the memory and computation consumption significantly, which enables an effective spatio-temporal learning directly from a tiny patch.

- We build a shifted self-attention to fully consider the motion effect of objects, which yields effective modeling of complicated *inter-frame* variances in the spatio-temporal representational learning. Furthermore, a clip encoder with a pure-Transformer structure is employed for frame-wise attention, which models complicated and long-term *inter-frame* relationships at a minimal extra cost.
- The shifted chunk Transformer with pure-Transformer outperforms previous state-of-the-art approaches on several action recognition benchmarks, including Kinectics-400 [18], Kinetics-600 [6], UCF101 [37] and HMDB51 [23].

2 Related Work

Conventional deep learning based action recognition Conventional deep spatio-temporal representational learning mainly involves two aspects: deep sequential learning based methods [26, 27] and deep ConvNet based methods [33, 14, 15]. The recurrent networks can be extended to 3D spatio-temporal domain for action recognition [26]. In deep ConvNet based methods, two-stream ConvNet employs two branches of 2D ConvNets and explicitly models motion by optical flow [36]. The C3D [39] and I3D [7] directly extend 2D ConvNets to 3D ConvNets, which is natural for 3D spatio-temporal representational learning [8]. However, the 3D ConvNet requires significantly more computation and more training data to achieve a desired accuracy [49]. Thus, P3D [32] and S3D [49] attempt to factorize the 3D convolution into a 2D spatial convolution and a 1D temporal convolution. SlowFast network [15] and X3D [14] conduct trade-offs among resolution, temporal frame rate and the number of channels for the efficient video recognition. Non-local network [47] proposes to add non-local operations in deep network and captures long-range dependencies. The recent pure-Transformer based spatio-temporal learning enables longer dependency relationship modeling and further increases the accuracy of action recognition [3].

Vision Transformers NLP community has witnessed the great success of pre-training by Transformer [42, 11], and it has been emerging for image classification [12, 38, 34], object detection [5], and image super-resolution [31]. CPVT [9] employs pre-defined and independent input tokens to increase the generalization for image classification. Pure-Transformer network has no inductive bias or prior as ConvNets. ViT [12] pre-trains on large amounts of data and attains excellent results on image classification. CvT [48] introduces convolutions into ViT to yield better performance and efficiency. DeiT [38] and MViT [13] instead employ distillation and multi-scale to cope with the training difficulty. PVT [45] and segmentation Transformer [51] further extend Transformer to dense prediction tasks, *e.g.*, object detection and semantic segmentation. Simply applying Transformer to 3D video spatio-temporal representational learning aggravates the training difficulty significantly, and it requires advanced model design for pure-Transformer based spatio-temporal learning.

Transformer based action recognition Recently, only a few works have been conducted using pure-Transformer for spatio-temporal learning [3, 13, 4, 1]. Most of the efforts focus on designing efficient Transformer models to reduce the computation and memory consumption. ViViT [3] and TimeSformer [4] study various factorization methods along spatial- and temporal-dimensions. MViT [13] conducts a trade-off between resolution and the number of channels, and constructs a multi-scale Transformer to learn a hierarchy from simple dense resolution and fine-grained features to complex coarse features. VATT [1] conducts unsupervised multi-modality self-supervised learning with a pure-Transformer structure. In this work, we extract fine-grained *intra-frame* features from each tiny patch and model complicated *inter-frame* relationship through efficient and advanced self-attention blocks.

3 Method

In this section, we describe each component of our shifted chunk Transformer for spatio-temporal representation learning in video based action recognition.

3.1 Overview

Let $\mathbf{X} = [\mathbf{X}_1, \mathbf{X}_2, \dots, \mathbf{X}_T] \in \mathbb{R}^{T \times H \times W \times 3}$ be one input clip of T RGB frames sampled from a video, where $\mathbf{X}_i \in \mathbb{R}^{H \times W \times 3}$ is the i -th frame in the clip, and H and W are the frame size. To design an efficient pure-Transformer based spatio-temporal learning, we construct a shifted chunk Transformer, including image chunk self-attention blocks, shifted multi-head self-attention blocks, and a clip encoder, as illustrated in Fig. 1. We first construct an image chunk self-attention block leveraging the advanced efficient Transformer design in NLP [20], which is illustrated in the left of Fig. 1. The locality-sensitive hashing (LSH) [2] in the image chunk self-attention enables a relatively small patch as a token, thus it is capable of extracting fine-grained *intra-frame* features. A linear pooling layer is designed to adaptively reduce the resolution after LSH attention. After that, a shifted self-attention is designed to extract motion related *inter-frame* features. Our shifted self-attention considers the motion of objects across nearby frames and explicitly models the temporal relationship into self-attention. The frame encoder shown in dark grey color can be an effective feature extractor which can be stacked for several times. The hierarchical frame encoder and image chunk self-attention further learns an effective multi-level feature from local to global abstraction. Lastly, we employ a pure-Transformer to learn complicated *inter-frame* relationships and frame-wise attention along the temporal dimension. We use multi-head self-attention (MSA) in all the blocks.

3.2 Image Chunk Self-Attention

Transformer can learn complicated long range dependencies which can be computed through the high efficient matrix product [42]. Different from convolution which has inherent inductive bias [12], Transformer learns the entire features from data. The main challenge for a pure-Transformer based vision model mainly involves two aspects: 1) how to design an efficient model to learn effective features from the entire image, because simply treating each pixel as a token is computationally intensive, 2) how to train this powerful model and learn various effective features from data. ViT [12] treats each patch of size 16×16 as one token and pre-trains the model with large amounts of data. We argue that Transformer with a smaller patch as a token can extract fine-grained features which improves spatio-temporal learning for action recognition. For ViT-B-16 [12] of crop size 224×224 as a frame encoder followed by a shifted MSA and a clip encoder, a smaller patch size of 8×8 yields better accuracy on Kinectics-400 and UCF101 as shown in Table 1.

The Transformer computes each pairwise correlation through a dot product, thus it has a high computational complexity of $O(L^2)$, where L is the totally number of tokens. In natural language processing (NLP), LSH attention [20] employs locality-sensitive hashing (LSH) bucketing [2] and chunk sorting for queries and keys to approximate the attention matrix computation. Leveraging the efficient LSH approximation, the LSH attention reduce the computation complexity to $O(L \log L)$.

To preserve locality property and learn transition and rotation invariant low-level features from images, we firstly design an image local chunk self-attention with shared parameters along different image local windows, or image chunks. Each image chunk consists of multiple tiny patches as illustrated in the left bottom block of Fig. 1. We intend to employ patches of a small size in the image local chunk self-attention which is the first level abstraction of the input, so that the model extracts a fine-grained

Table 1: ViT-B [12] with a smaller patch size yields higher accuracy (%).

Crop size	Patch size	K400	UCF101
224	16	75.3	95.3
224	8	78.4	97.0

representation which enhances the entire spatial-temporal learning. Employing the small patch yields large number of tokens in the following self-attention, and we construct an image locality-sensitive hashing (LSH) attention leveraging advanced design of Transformer in NLP [20]. The image LSH attention can efficiently extract higher-level and plentiful *intra-frame* features ranging from a tiny patch to the entire image. The framework of image chunk self-attention is illustrated in the left part of Fig. 1.

Image local chunk self-attention In the shifted chunk Transformer, we firstly construct an image local chunk self-attention which slides one self-attention for each tiny patch along the whole image. The local chunk self-attention is illustrated in the bottom block of Fig. 1. Let h, w be the height and width of the tiny image patch $\mathbf{p} \in \mathbb{R}^{h \times w \times 3}$. Following the success of ViT [12], we treat each patch as one dimensional vector of length $h \times w \times 3$. Suppose each chunk consists of $m \times n$ tiny patches, denoted as $\{\mathbf{p}_{1,1}, \mathbf{p}_{1,2}, \dots, \mathbf{p}_{1,n}; \mathbf{p}_{2,1}, \dots, \mathbf{p}_{2,n}; \dots; \mathbf{p}_{m,1}, \dots, \mathbf{p}_{m,n}\}$. After flattening the chunk into a list of tiny patches, we denote the chunk as $\{\mathbf{p}_1, \mathbf{p}_2, \dots, \mathbf{p}_L\}$ without loss of generality, where $L = m \times n$.

In image local chunk self-attention, we use a standard learnable 1D position embedding $\mathbf{E}_{pos} \in \mathbb{R}^{L \times D}$ to retain position information as

$$\mathbf{z}_0 = [\mathbf{p}_1 \mathbf{E}; \mathbf{p}_2 \mathbf{E}; \dots; \mathbf{p}_{m \times n} \mathbf{E}] + \mathbf{E}_{pos}, \quad \mathbf{E} \in \mathbb{R}^{(h \times w \times 3) \times D}, \quad (1)$$

where \mathbf{E} is the linear patch embedding matrix, and D is the embedding dimension. Then we can construct alternating layers of multi-head self-attention (MSA), MLP with GELU [17] non-linearity, Layernorm (LN) and residual connections [42] for the chunk as

$$\mathbf{z}'_m = \text{MSA}(\text{LN}(\mathbf{z}_{m-1})) + \mathbf{z}_{m-1}, \quad \mathbf{z}_m = \text{MLP}(\text{LN}(\mathbf{z}'_m)) + \mathbf{z}'_m, \quad m = 1, \dots, M, \quad (2)$$

where M is the number of blocks. We conduct the image local chunk self-attention sliding the entire image without overlapping. The parameters of the image local chunk self-attention are shared among all the image chunks, which forces the chunk self-attention to learn translation and rotation invariant, and fine-grained features. The tiny patch-wise feature extraction preserves the locality property, which is a strong prior for natural images. After the image local chunk self-attention, we obtain the extracted features for the entire image denoted as $\mathbf{y} = [\mathbf{y}_1; \mathbf{y}_2; \dots; \mathbf{y}_L; \dots; \mathbf{y}_{L \times L}]$, where the entire image can be split into $L' = m' \times n' = \lceil \frac{H}{h \times m} \rceil \times \lceil \frac{W}{w \times n} \rceil$ chunks, and we conduct zero padding for the last chunks in each row and column.

The image local chunk self-attention scheme forces to learn image locality features which is a desired property for a low-level feature extractor [24]. For pure-Transformer based vision system, it also reduces the memory consumption significantly because it restricts the correlation of one tiny patch within the local chunk. Therefore, the memory and computational complexity of dot-product attention in image local chunk self-attention can be reduced to $O(L^2)$ compared to the complexity of conventional self-attention $O((L' \times L)^2)$.

Image locality-sensitive hashing (LSH) attention After image local chunk self-attention blocks, we obtain local fine-grained features of length $L' \times L$. Since the patch size is tiny, the total number of patches can be large, which leads to more difficult training than other vision Transformers [3, 12]. In NLP, LSH attention [20] is proposed to handle quite long sequence data, which employs locality-sensitive hashing (LSH) bucketing approximation and bucket sorting to reduce the computational complexity of matrix product between query and key in self-attention.

In dot-product attention, the softmax activation function pushes the attention weights close to 1 or 0, which means the attention matrix is typically sparse. The query and key can be approximated by locality-sensitive hashing (LSH) [2] to reduce the computational complexity. Furthermore, through bucketing sort, the attention matrix product can be accelerated by a chunk triangular matrix product, which has been validated by LSH attention [20].

The used multi-head image LSH attention can be constructed as

$$\mathbf{y}' = \text{MSA}(\text{LSHAtt}(\text{LN}(\mathbf{y}))) + \mathbf{y}, \quad \mathbf{s} = \text{MLP}(\text{LN}(\mathbf{y}')) + \mathbf{y}', \quad (3)$$

where LSH attention $\text{LSHAtt}(\cdot)$ employs angular distance to conduct LSH hashing [2]. The image LSH attention reduces the memory and time complexity to $O(L' \times L \log(L' \times L))$, compared with that of conventional dot-product attention $O((L' \times L)^2)$. The image LSH attention reduces the complexity significantly because the patch size is tiny and the number of tiny patches $L' \times L$ are large. The image level LSH attention in the second level learns relatively global features from the first level’s local fine-grained features.

The hierarchical feature learning from local to global has been validated as an effective principle for vision system design [24, 43]. Inspired by hierarchical abstraction in ConvNets [24], we construct a linear pooling layer which firstly conducts squeeze then employs linear projection for feature dimension reduction. The linear pooling adaptively squeezes the sequence length by $\frac{1}{4}$.

$$\begin{aligned}
\text{Reshape: } \mathbf{s} &= [\mathbf{s}_{1,1}, \dots, \mathbf{s}_{1,n \times n'}; \dots; \mathbf{s}_{m \times m',1}, \dots, \mathbf{s}_{m \times m',n \times n'}], \\
\text{Squeeze: } \mathbf{s}' &= [\mathbf{s}'_{1,1}, \dots, \mathbf{s}'_{1,n \times n' / 2}; \dots; \mathbf{s}'_{m \times m' / 2,1}, \dots, \mathbf{s}'_{m \times m' / 2, n \times n' / 2}], \\
\text{Linear: } \mathbf{t} &= [\mathbf{s}'_{1,1} \mathbf{E}_t, \dots, \mathbf{s}'_{1,n \times n' / 2} \mathbf{E}_t; \dots; \mathbf{s}'_{m \times m' / 2,1} \mathbf{E}_t, \dots, \mathbf{s}'_{m \times m' / 2, n \times n' / 2} \mathbf{E}_t],
\end{aligned} \tag{4}$$

where $\mathbf{s}'_{i,j}$ in \mathbf{s}' concatenates $\mathbf{s}_{2i-1,2j-1}$, $\mathbf{s}_{2i-1,2j}$, $\mathbf{s}_{2i,2j-1}$ and $\mathbf{s}_{2i,2j}$ from \mathbf{s} , \mathbf{E}_t is the linear projection matrix to adaptively reduce the number of dimensions after squeeze by half. The reshape is to retain the spatial relationship of each patch, and the squeeze reduces the number of patches by $\frac{1}{4}$ and enlarges the feature dimensions by four times. The linear pooling layer forces the model to learn high-level global features in the following layers.

3.3 Shifted Multi-Head Self-Attention

Considering the motion effect of objects, we explicitly construct a shifted multi-head self-attention (MSA) for spatio-temporal learning after image chunk self-attention as illustrated in Fig. 1. For video classification, a special classification token ([CLS]) [11] can be prepended into the feature sequence. To learn frame-wise spatio-temporal representations, we prepend the [CLS] token to each frame. Without loss of generality, we denote the image chunk self-attention feature to be a list of $[\mathbf{t}_{i,1}; \mathbf{t}_{i,2}; \dots; \mathbf{t}_{i,L \times L' / 4}]$ for the i -th frame. Then, we obtain the input of T frames for shifted MSA as

$$\begin{aligned}
\mathbf{t}' &= [\mathbf{t}'_{1,1}; \dots; \mathbf{t}'_{1,1+L \times L' / 4}; \dots; \mathbf{t}'_{T,1}; \dots; \mathbf{t}'_{T,1+L \times L' / 4}] \\
&= [\mathbf{z}_{1,cls}; \mathbf{t}_{1,1}; \dots; \mathbf{t}_{1,L \times L' / 4}; \dots; \mathbf{z}_{T,cls}; \mathbf{t}_{T,1}; \dots; \mathbf{t}_{T,L \times L' / 4}].
\end{aligned} \tag{5}$$

The shifted multi-head self-attention explicitly considers the *inter-frame* motion of objects, which computes the correlation between the current frame and the previous frame in the attention matrix, which can be formulated as

$$\mathbf{q}_{t,p}^i = \text{LN}(\mathbf{t}'_{t,p}) \mathbf{W}_Q^i, \quad \mathbf{k}_{t,p}^i = \text{LN}(\mathbf{t}'_{t-1,p}) \mathbf{W}_K^i, \quad \mathbf{v}_{t,p}^i = \text{LN}(\mathbf{t}'_{t,p}) \mathbf{W}_V^i, \tag{6}$$

where \mathbf{W}_Q^i , \mathbf{W}_K^i and \mathbf{W}_V^i are projection matrices for head i , and we employ a cyclic way to calculate the key of the first frame $t = 1$ by defining $\mathbf{t}'_{0,p} = \mathbf{t}'_{T,p}$. By concatenating $\mathbf{q}_{t,p}^i$, $\mathbf{k}_{t,p}^i$, $\mathbf{v}_{t,p}^i$ into matrices \mathbf{Q}_t^i , \mathbf{K}_t^i , \mathbf{V}_t^i along patch location p , the shifted MSA for frame t can be calculated as

$$\begin{aligned}
\mathbf{a}_t &= \text{Concat}(\text{Attention}(\mathbf{Q}_t^1, \mathbf{K}_t^1, \mathbf{V}_t^1), \dots, \text{Attention}(\mathbf{Q}_t^l, \mathbf{K}_t^l, \mathbf{V}_t^l)) \mathbf{W}_O, \\
\mathbf{a}'_t &= \text{MLP}(\text{LN}(\mathbf{a}_t)) + \mathbf{a}_t,
\end{aligned} \tag{7}$$

where l is the number of heads in multi-head self-attention. The shifted self-attention compensates object motion and spatial variances. We explicitly integrate motion shift into self-attention, which extracts robust features for spatio-temporal learning. The block with alternating layers of image chunk self-attention and shifted MSA can be stacked for multiple times to fully extract effective hierarchical fine-grained features from tiny local patches to the whole clip in our shifted chunk Transformer.

Table 2: Hyper-parameters of data processing and optimization.

	K400	K600	U101	H51	MMT
Frame Rate	5	5	10	10	8
Frame Stride	10	10	8	8	10
#Warmup epochs	2	2	3	4	2
Learning rate	0.3	0.3	0.25	0.25	0.3
Label smoothing	0.1	0.1	0	0	0.3
Dropout	0.2	0.2	0	0	0.2

3.4 Clip Encoder for Global Clip Attention

To learn complicated *inter-frame* relationship from the extracted frame-level features, we design a clip encoder based on a pure-Transformer structure to adaptively learn frame-wise attention. To facilitate the video classification, we prepend a global special classification token ([CLS]) into the frame-level feature sequence. In this module, we employ the classification feature \mathbf{a}'_{t_1} corresponding to $\mathbf{z}_{t,cls}$ as the frame-level feature for frame t . To consider frame position, we also employ a standard learnable 1D position embedding as each frame position embedding. The clip encoder can be formulated as

$$\begin{aligned}
 \mathbf{b}_0 &= [\mathbf{b}_{cls}; \mathbf{a}'_{1_1}\mathbf{E}'; \dots; \mathbf{a}'_{T_1}\mathbf{E}'] + \mathbf{E}'_{pos}, \quad \mathbf{E}'_{pos} \in \mathbb{R}^{(T+1) \times D'}, \\
 \mathbf{b}'_m &= \text{MSA}(\text{LN}(\mathbf{b}_{m-1})) + \mathbf{b}_{m-1}, \quad \mathbf{b}_m = \text{MLP}(\text{LN}(\mathbf{b}'_m)) + \mathbf{b}'_m, \quad m = 1, \dots, M', \\
 \mathbf{c} &= \text{MLP}(\text{LN}(\mathbf{b}_{M'_1}))
 \end{aligned} \tag{8}$$

where \mathbf{E}' is the linear frame embedding matrix, D' is the clip encoder embedding size, M' is the number of blocks, and $\mathbf{b}_{M'_1}$ is the clip-level classification feature corresponding to classification token \mathbf{b}_{cls} , \mathbf{c} is the video classification logit for softmax. We use dropout [22] for the second last layer and cross-entropy loss with label smoothing [30] for training. The clip encoder can be efficient with a minimal computational cost as show in the Appendix to achieve a powerful *inter-frame* representation learning.

4 Experiment

We evaluate our shifted chunk Transformer, denoted as SCT, on five commonly used action recognition datasets: Kinetics-400 [18], Kinetics-600 [6], Moment-in-Time [29] (Appendix), UCF101 [37] and HMDB51 [23]. We adopt ImageNet-21K for the pre-training [35, 10] because of large model capacity of SCT. The default patch size for each image token is 4×4 . In the training, we use a synchronous stochastic gradient descent with momentum of 0.9, a cosine annealing schedule [28], and the number of epochs of 50. We use batch size of 32, 16 and 8 for SCT-S, SCT-M and SCT-L, respectively. And the frame crop size is set to be 224×224 . For data augmentation, we randomly select the start frame to generate the input clip. In the inference, we extract multiple views from each video and ensemble predictions from these views to obtain the final result by averaging the softmax probabilistic scores from these multi-view predictions. The details of initial learning rate, optimization and data processing are shown in Table 2. All the experiments are run on 8 NVIDIA Tesla V100 32 GB GPU cards.

We construct three shifted chunk Transformers, SCT-S, SCT-M, and SCT-L, in terms of various model sizes and computation complexities. We employ four consecutive blocks with alternating one image chunk self-attention and one shifted MSA. The patch embedding size D , MLP dimension of these self-attentions, the number of image local chunk self-attention layers M , the clip encoder embedding size D' , MLP dimension of clip encoder, the numbers of heads in image local chunk self-attention, LSH attention, shifted MSA and clip encoder are shown in Table 3. Each image chunk self-attention consists of M layers image local chunk self-attention followed by an image LSH attention and a linear

Table 3: The model structure of three shifted chunk Transformers.

Model	D	MLP size	M	D'	Clip MLP size	#Heads	#Param	GFLOPs
SCT-S	96	384	4	192	768	[4 6 8 8]	18.72M	88.18
SCT-M	128	512	6	192	768	[4 8 8 8]	33.48M	162.90
SCT-L	192	768	4	192	768	[4 6 8 8]	59.89M	342.58

Table 4: The effect of frame extractor and the number of tokens on Top-1 accuracy (%).

Method	Patch size	Chunk size	#Tokens	#Param	GFLOPs	Kinetics-400
ViT-B-16	16	-	196	114.25M	405.06	75.33
ViT-B-16	12	-	784	114.25M	665.78	77.12
ViT-B-16	8	-	784	114.25M	1603.67	78.95
ViT-L-16	16	-	196	328.63M	1413.45	79.15
SCT-S	4	49	64	18.72M	88.18	78.41
SCT-M	4	49	64	33.48M	162.90	81.26
SCT-L	4	49	64	59.89M	342.58	83.02

pooling layer to reduce the number of spatial dimensions. We use four-layer clip encoders to obtain the video classification results as validated in the Appendix.

Validating frame feature extractor We compare the frame encoder of our shifted chunk Transformer (SCT) with ViT [12] in Table 4. For a fair comparison, we only replace the image local chunk self-attention with ViT, and remain all other components the same. From Table 4, we observe that 1) large models, ViT-L-16 and SCT-L, yield higher accuracy than base models, ViT-B-16 and SCT-S; 2) ViT with a small patch size achieves better accuracy than ViT with a large patch; 3) SCT-L improves the accuracy of ViT-L by 4% while using much less number of parameters and FLOPs. The tiny patch and enforced locality prior in image local chunk self-attention are validated to be effective for spatio-temporal learning.

Effect of shifted MSA We conduct experiments on Kinectis-400 and UCF101 to validate the hyper-parameters of the shifted MSA layer, including the number of shifted MSA layers, and the number of shifted frames used in the calculation of key in equation (6). All other network configurations follow the Table 3. The #Shifted MSA of 0 and #Shifted frame of 0 in Table 5 mean that one standard MSA is used instead of shifted MSA. From Table 5, we observe that 1) a shifted MSA improves the accuracy up to 1.5% compared with the conventional MSA; 2) one layer shifted MSA with the shifted number of frames of one yields the best accuracy. The shifted MSA explicitly formulates the motion effect of object by considering the nearby frames, which improves the accuracy for video classification. We use one layer shifted MSA with the number of shifted frames of one in our experiment.

Varying the number of input frames and temporal views In our experiments so far, we have kept the number of input frames fixed to 24 across different datasets. To discuss the effect of the number of input frames on video level inference accuracy, we validate the number of input frames of 24, 48, 96, and the number of temporal views from 1 to 6. Fig. 2 shows that as we increase the number of frames, the accuracy using a single clip increases, since the network is incorporated longer temporal information. However, as the number of used views increases, the accuracy difference is reduced. We use the number of frames of 24 and the number of temporal views of 4 in our experiment.

Table 5: The effect of the number of shifted MSA layers and the number of shifted frames on Top-1 accuracy (%).

Method	#Shifted MSA	#Shifted frame	K400	U101
SCT-S	0	0	76.91	97.01
SCT-S	1	1	78.41	98.02
SCT-S	1	5	77.02	97.15
SCT-S	2	1	77.45	97.33



Figure 3: Visualization of the patch and frame attention maps (the second and fourth rows).

Patch and frame attention Our shifted chunk Transformer (SCT) can detect fine-grained discriminative regions for each frame in the entire clip in Fig. 3. The designed framework of SCT leads to an easy diagnosis and explanation for the prediction, which potentially makes SCT applicable to various critical fields such as healthcare and autonomous driving.

Comparison to state-of-the-art approaches

We compare our shifted chunk Transformer (SCT) to the current state-of-the-art approaches based on the best hyper-parameters validated in the previous ablation studies. We obtain the results of previous state-of-the-art approaches from their papers.

Our shifted chunk Transformers (SCT) surpass previous state-of-the-art approaches including both recent Transformer based video classification and previous deep ConvNets based methods by 2.7%, 1.3%, 1.7% and 8.9% on Kinectis-400, Kinectic-600, UCF101 and HMDB51 in Table 6-7 based

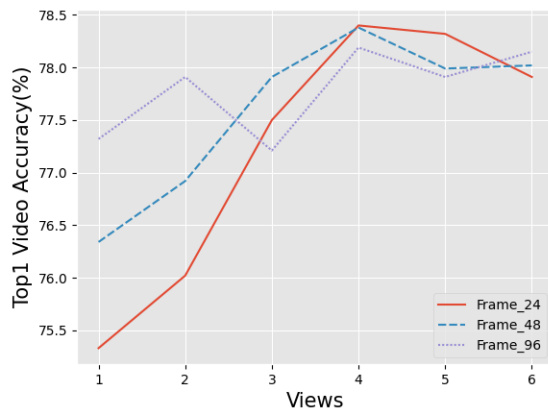


Figure 2: The effect of varying the number of input frames and temporal views.

Table 6: Top-1 and Top-5 accuracy (%) comparisons to state-of-the-art approaches on Kinectics-400.

Method	GFLOPs×Views	#Param	Top1	Top5
TEA [25]	70×10×3	-	76.1	92.5
I3D NL [47]	-	54M	77.7	93.3
CorrNet-101 [44]	224×10×3	-	79.2	-
ip-CSN-152 [40]	109×10×3	33M	79.2	93.8
SlowFast [15]	234×10×3	60M	79.8	93.9
X3D-XXL [14]	194×10×3	20M	80.4	94.6
TimeSformer [4]	2380×1×3	121M	80.7	94.7
MViT-B 64×3 [13]	455×3×3	37M	81.2	95.1
ViViT-L [3]	3992×4×3	89M	81.3	94.7
SCT-S	88×4×3	19M	78.4	93.8
SCT-M	163×4×3	33M	81.3	94.5
SCT-L	343×4×3	60M	83.0	95.4

Table 7: Classification accuracy (%) comparisons to state-of-the-art approaches on Kinectics-600, UCF101 (3 splits) and HMDB51 (3 splits). ‘K400’ denotes pretraining on Kinetics-400 and ImageNet. ‘K600’ denotes pretraining on Kinetics-600 and ImageNet.

Method	Views	#Para	Top1	Top5	Method	Pretrain	U101	H51
AttenNAS [46]	-	-	79.8	94.4	I3D [7]	K400	95.4	74.5
LGD-3D [33]	-	-	81.5	95.6	ResNeXt [16]	K400	94.5	70.2
SlowFast [15]	10×3	60M	81.8	95.1	R(2+1)D [41]	K400	96.8	74.5
X3D-XL [14]	10×3	11M	81.9	95.5	S3D-G [49]	K400	96.8	75.9
TimeSformer [4]	1×3	121M	82.4	96.0	LGD-3D [33]	K600	97.0	75.7
ViViT-L [3]	4×3	89M	83.0	95.7	SCT-S	ImageNet	98.0	76.5
SCT-S	4×3	19M	77.5	93.1	SCT-L	ImageNet	97.7	81.4
SCT-M	4×3	33M	81.7	95.5	SCT-S	K400	98.3	81.5
SCT-L	4×3	60M	84.3	96.3	SCT-M	K400	98.5	83.2
					SCT-L	K400	98.7	84.6

on RGB frames, respectively. The local scheme and LSH approximation in image chunk self-attention enables to use patches of a small size. Because of the efficient model design, SCT achieves the best accuracy even only using pretraining on the ImageNet on UCF101 and HMDB51. Besides the higher action recognition accuracy, the SCT employs less number of parameters and FLOPs than ViViT because we employ less number of channels and our SCT is effective for spatio-temporal learning.

5 Conclusion

In this work, we proposed a new spatio-temporal learning called shifted chunk Transformer inspired by the recent success of vision Transformer in image classification. However, the current pure-Transformer based spatio-temporal learning is limited by computational efficiency and feature robustness. To address these challenges, we propose several efficient and powerful components for spatio-temporal Transformer, which is able to learn fine-grained features from a tiny image patch and model complicated spatio-temporal dependencies. We construct an image chunk self-attention which leverages locality-sensitive hashing to efficiently capture fine-grained local representation with a relatively low computation cost. Our shifted self-attention can effectively model complicated *inter-frame* variances. Furthermore, we build a clip encoder based on pure-Transformer for frame-wise attention and long-term *inter-frame*

dependency modeling. We conduct thorough ablation studies to validate each component and hyper-parameters in our shifted chunk Transformer. It outperforms previous state-of-the-art approaches including both pure-Transformer architectures and deep 3D convolutional networks on Kinetics-400, Kinetics-600, UCF101 and HMDB51 datasets in terms of accuracy and efficiency. For future work, employing neural architecture search to explore optimal architectures based on our shifted chunk Transformer for efficient and powerful spatio-temporal learning is a promising topic.

References

- [1] Hassan Akbari, Linagzhe Yuan, Rui Qian, Wei-Hong Chuang, Shih-Fu Chang, Yin Cui, and Boqing Gong. Vatt: Transformers for multimodal self-supervised learning from raw video, audio and text. *arXiv preprint arXiv:2104.11178*, 2021.
- [2] Alexandr Andoni, Piotr Indyk, TMM Laarhoven, Ilya Razenshteyn, and Ludwig Schmidt. Practical and optimal lsh for angular distance. In *Advances in Neural Information Processing Systems (NIPS 2015)*, pages 1225–1233. Curran Associates, 2015.
- [3] Anurag Arnab, Mostafa Dehghani, Georg Heigold, Chen Sun, Mario Lučić, and Cordelia Schmid. Vivit: A video vision transformer. *arXiv preprint arXiv:2103.15691*, 2021.
- [4] Gedas Bertasius, Heng Wang, and Lorenzo Torresani. Is space-time attention all you need for video understanding? *arXiv preprint arXiv:2102.05095*, 2021.
- [5] Nicolas Carion, Francisco Massa, Gabriel Synnaeve, Nicolas Usunier, Alexander Kirillov, and Sergey Zagoruyko. End-to-end object detection with transformers. In *European Conference on Computer Vision*, pages 213–229. Springer, 2020.
- [6] Joao Carreira, Eric Noland, Andras Banki-Horvath, Chloe Hillier, and Andrew Zisserman. A short note about kinetics-600. *arXiv preprint arXiv:1808.01340*, 2018.
- [7] Joao Carreira and Andrew Zisserman. Quo vadis, action recognition? a new model and the kinetics dataset. In *proceedings of the IEEE Conference on Computer Vision and Pattern Recognition*, pages 6299–6308, 2017.
- [8] R Christoph and Feichtenhofer Axel Pinz. Spatiotemporal residual networks for video action recognition. *Advances in Neural Information Processing Systems*, pages 3468–3476, 2016.
- [9] Xiangxiang Chu, Bo Zhang, Zhi Tian, Xiaolin Wei, and Huaxia Xia. Do we really need explicit position encodings for vision transformers? *arXiv preprint arXiv:2102.10882*, 2021.
- [10] Jia Deng, Wei Dong, Richard Socher, Li-Jia Li, Kai Li, and Li Fei-Fei. Imagenet: A large-scale hierarchical image database. In *2009 IEEE Conference on Computer Vision and Pattern Recognition*, pages 248–255. Ieee, 2009.
- [11] Jacob Devlin, Ming-Wei Chang, Kenton Lee, and Kristina Toutanova. Bert: Pre-training of deep bidirectional transformers for language understanding. In *Proceedings of the 2019 Conference of the North American Chapter of the Association for Computational Linguistics: Human Language Technologies, Volume 1 (Long and Short Papers)*, pages 4171–4186, 2019.
- [12] Alexey Dosovitskiy, Lucas Beyer, Alexander Kolesnikov, Dirk Weissenborn, Xiaohua Zhai, Thomas Unterthiner, Mostafa Dehghani, Matthias Minderer, Georg Heigold, Sylvain Gelly, et al. An image is worth 16x16 words: Transformers for image recognition at scale. In *International Conference on Learning Representations*, 2021.
- [13] Haoqi Fan, Bo Xiong, Karttikeya Mangalam, Yanghao Li, Zhicheng Yan, Jitendra Malik, and Christoph Feichtenhofer. Multiscale vision transformers. *arXiv preprint arXiv:2104.11227*, 2021.

- [14] Christoph Feichtenhofer. X3d: Expanding architectures for efficient video recognition. In *Proceedings of the IEEE/CVF Conference on Computer Vision and Pattern Recognition*, pages 203–213, 2020.
- [15] Christoph Feichtenhofer, Haoqi Fan, Jitendra Malik, and Kaiming He. Slowfast networks for video recognition. In *Proceedings of the IEEE/CVF International Conference on Computer Vision*, pages 6202–6211, 2019.
- [16] Kensho Hara, Hirokatsu Kataoka, and Yutaka Satoh. Can spatiotemporal 3d cnns retrace the history of 2d cnns and imagenet? In *Proceedings of the IEEE Conference on Computer Vision and Pattern Recognition*, pages 6546–6555, 2018.
- [17] Dan Hendrycks and Kevin Gimpel. Gaussian error linear units (gelus). *arXiv preprint arXiv:1606.08415*, 2016.
- [18] Will Kay, Joao Carreira, Karen Simonyan, Brian Zhang, Chloe Hillier, Sudheendra Vijayanarasimhan, Fabio Viola, Tim Green, Trevor Back, Paul Natsev, et al. The kinetics human action video dataset. *arXiv preprint arXiv:1705.06950*, 2017.
- [19] Qihong Ke, Mario Fritz, and Bernt Schiele. Time-conditioned action anticipation in one shot. In *Proceedings of the IEEE/CVF Conference on Computer Vision and Pattern Recognition*, pages 9925–9934, 2019.
- [20] Nikita Kitaev, Łukasz Kaiser, and Anselm Levskaya. Reformer: The efficient transformer. In *International Conference on Learning Representations*, 2020.
- [21] Matej Kristan, Jiri Matas, Ales Leonardis, Michael Felsberg, Roman Pflugfelder, Joni-Kristian Kamarainen, Luka Cehovin Zajc, Ondrej Drbohlav, Alan Lukezic, Amanda Berg, et al. The seventh visual object tracking vot2019 challenge results. In *Proceedings of the IEEE/CVF International Conference on Computer Vision Workshops*, pages 0–0, 2019.
- [22] Alex Krizhevsky, Ilya Sutskever, and Geoffrey E Hinton. Imagenet classification with deep convolutional neural networks. *Advances in Neural Information Processing Systems*, 25:1097–1105, 2012.
- [23] Hildegard Kuehne, Hueihan Jhuang, Estíbaliz Garrote, Tomaso Poggio, and Thomas Serre. Hmdb: a large video database for human motion recognition. In *International Conference on Computer Vision*, pages 2556–2563. IEEE, 2011.
- [24] Yann LeCun, Léon Bottou, Yoshua Bengio, and Patrick Haffner. Gradient-based learning applied to document recognition. *Proceedings of the IEEE*, 86(11):2278–2324, 1998.
- [25] Yan Li, Bin Ji, Xintian Shi, Jianguo Zhang, Bin Kang, and Limin Wang. Tea: Temporal excitation and aggregation for action recognition. In *Proceedings of the IEEE/CVF Conference on Computer Vision and Pattern Recognition*, pages 909–918, 2020.
- [26] Jun Liu, Amir Shahroudy, Dong Xu, and Gang Wang. Spatio-temporal lstm with trust gates for 3d human action recognition. In *European Conference on Computer Vision*, pages 816–833. Springer, 2016.
- [27] Jun Liu, Gang Wang, Ping Hu, Ling-Yu Duan, and Alex C Kot. Global context-aware attention lstm networks for 3d action recognition. In *Proceedings of the IEEE Conference on Computer Vision and Pattern Recognition*, pages 1647–1656, 2017.
- [28] Ilya Loshchilov and Frank Hutter. Sgdr: Stochastic gradient descent with warm restarts. In *International Conference on Learning Representations*, 2017.

- [29] Mathew Monfort, Alex Andonian, Bolei Zhou, Kandan Ramakrishnan, Sarah Adel Bargal, Tom Yan, Lisa Brown, Quanfu Fan, Dan Gutfreund, Carl Vondrick, et al. Moments in time dataset: one million videos for event understanding. *IEEE Transactions on Pattern Analysis and Machine Intelligence*, 42(2):502–508, 2019.
- [30] Rafael Müller, Simon Kornblith, and Geoffrey Hinton. When does label smoothing help? In *Advances in Neural Information Processing Systems*, 2019.
- [31] Niki Parmar, Ashish Vaswani, Jakob Uszkoreit, Lukasz Kaiser, Noam Shazeer, Alexander Ku, and Dustin Tran. Image transformer. In *International Conference on Machine Learning*, pages 4055–4064. PMLR, 2018.
- [32] Zhaofan Qiu, Ting Yao, and Tao Mei. Learning spatio-temporal representation with pseudo-3d residual networks. In *proceedings of the IEEE International Conference on Computer Vision*, pages 5533–5541, 2017.
- [33] Zhaofan Qiu, Ting Yao, Chong-Wah Ngo, Xinmei Tian, and Tao Mei. Learning spatio-temporal representation with local and global diffusion. In *Proceedings of the IEEE/CVF Conference on Computer Vision and Pattern Recognition*, pages 12056–12065, 2019.
- [34] Prajit Ramachandran, Niki Parmar, Ashish Vaswani, Irwan Bello, Anselm Levskaya, and Jonathon Shlens. Stand-alone self-attention in vision models. In *Advances in Neural Information Processing Systems*, 2019.
- [35] Tal Ridnik, Emanuel Ben-Baruch, Asaf Noy, and Lihi Zelnik-Manor. Imagenet-21k pretraining for the masses. *arXiv preprint arXiv:2104.10972*, 2021.
- [36] Karen Simonyan and Andrew Zisserman. Two-stream convolutional networks for action recognition in videos. In *Proceedings of the 27th International Conference on Neural Information Processing Systems-Volume 1*, pages 568–576, 2014.
- [37] Khurram Soomro, Amir Roshan Zamir, and Mubarak Shah. Ucf101: A dataset of 101 human actions classes from videos in the wild. *arXiv preprint arXiv:1212.0402*, 2012.
- [38] Hugo Touvron, Matthieu Cord, Matthijs Douze, Francisco Massa, Alexandre Sablayrolles, and Hervé Jégou. Training data-efficient image transformers & distillation through attention. *arXiv preprint arXiv:2012.12877*, 2020.
- [39] Du Tran, Lubomir Bourdev, Rob Fergus, Lorenzo Torresani, and Manohar Paluri. Learning spatiotemporal features with 3d convolutional networks. In *Proceedings of the IEEE International Conference on Computer Vision*, pages 4489–4497, 2015.
- [40] Du Tran, Heng Wang, Lorenzo Torresani, and Matt Feiszli. Video classification with channel-separated convolutional networks. In *Proceedings of the IEEE/CVF International Conference on Computer Vision*, pages 5552–5561, 2019.
- [41] Du Tran, Heng Wang, Lorenzo Torresani, Jamie Ray, Yann LeCun, and Manohar Paluri. A closer look at spatiotemporal convolutions for action recognition. In *Proceedings of the IEEE Conference on Computer Vision and Pattern Recognition*, pages 6450–6459, 2018.
- [42] Ashish Vaswani, Noam Shazeer, Niki Parmar, Jakob Uszkoreit, Llion Jones, Aidan N Gomez, Lukasz Kaiser, and Illia Polosukhin. Attention is all you need. In *Advances in Neural Information Processing Systems*, volume 30, pages 5998–6008, 2017.
- [43] Andrea Vedaldi and Brian Fulkerson. Vlfeat: An open and portable library of computer vision algorithms. In *Proceedings of the 18th ACM International Conference on Multimedia*, pages 1469–1472, 2010.

- [44] Heng Wang, Du Tran, Lorenzo Torresani, and Matt Feiszli. Video modeling with correlation networks. In *Proceedings of the IEEE/CVF Conference on Computer Vision and Pattern Recognition*, pages 352–361, 2020.
- [45] Wenhai Wang, Enze Xie, Xiang Li, Deng-Ping Fan, Kaitao Song, Ding Liang, Tong Lu, Ping Luo, and Ling Shao. Pyramid vision transformer: A versatile backbone for dense prediction without convolutions. *arXiv preprint arXiv:2102.12122*, 2021.
- [46] Xiaofang Wang, Xuehan Xiong, Maxim Neumann, AJ Piergiovanni, Michael S Ryoo, Anelia Angelova, Kris M Kitani, and Wei Hua. Attentionnas: Spatiotemporal attention cell search for video classification. In *European Conference on Computer Vision*, pages 449–465. Springer, 2020.
- [47] Xiaolong Wang, Ross Girshick, Abhinav Gupta, and Kaiming He. Non-local neural networks. In *Proceedings of the IEEE Conference on Computer Vision and Pattern Recognition*, pages 7794–7803, 2018.
- [48] Haiping Wu, Bin Xiao, Noel Codella, Mengchen Liu, Xiyang Dai, Lu Yuan, and Lei Zhang. Cvt: Introducing convolutions to vision transformers. *arXiv preprint arXiv:2103.15808*, 2021.
- [49] Saining Xie, Chen Sun, Jonathan Huang, Zhuowen Tu, and Kevin Murphy. Rethinking spatiotemporal feature learning: Speed-accuracy trade-offs in video classification. In *Proceedings of the European Conference on Computer Vision (ECCV)*, pages 305–321, 2018.
- [50] Serena Yeung, Olga Russakovsky, Greg Mori, and Li Fei-Fei. End-to-end learning of action detection from frame glimpses in videos. In *Proceedings of the IEEE Conference on Computer Vision and Pattern Recognition*, pages 2678–2687, 2016.
- [51] Sixiao Zheng, Jiachen Lu, Hengshuang Zhao, Xiatian Zhu, Zekun Luo, Yabiao Wang, Yanwei Fu, Jianfeng Feng, Tao Xiang, Philip HS Torr, et al. Rethinking semantic segmentation from a sequence-to-sequence perspective with transformers. In *Proceedings of the IEEE/CVF Conference on Computer Vision and Pattern Recognition*, 2021.

A Appendix

Varying the number of clip encoder layers See Table 8. From the table, adding two more layers of clip encoder only increases the number of parameters by 1M. The clip encoder using four layers yields better accuracy. We use four layered clip encoder in our experiment.

Table 8: Effect of clip encoder on the Top-1 accuracy (%)

Name	#Layer	#Param	FLOPs	K400	U101
SCT-S	2	17.67M	86.14G	76.32	97.35
SCT-S	4	18.72M	88.18G	78.41	98.02

Pretrained Model Analysis See Table 9. Pretraining on large amount of data yields better top-1 accuracy.

Table 9: Pretrain Model Result

UCF101		
Name	Pretrain Type	Top-1 Acc
SCT-S	ImageNet	98.02%
SCT-M	ImageNet	97.45 %
SCT-L	ImageNet	97.70 %
SCT-S	ImageNet+Kinetics-400	98.33 %
SCT-M	ImageNet+Kinetics-400	98.45 %
SCT-L	ImageNet+Kinetics-400	98.71 %
HMDB51		
SCT-S	ImageNet	76.52 %
SCT-M	ImageNet	78.31 %
SCT-L	ImageNet	81.42 %
SCT-S	ImageNet+Kinetics-400	81.54 %
SCT-M	ImageNet+Kinetics-400	83.22 %
SCT-L	ImageNet+Kinetics-400	84.61 %

Results on Moments in Time [29] See Table 10. We achieve comparable accuracy with much less number of parameters and GFLOPs on Moments in Time [29].

Table 10: Results on Moments in Time [29]

Method	#Param	GFLOPs	Top-1 (%)	Top-5 (%)
I3D [7]	25M	-	29.5	56.1
ViViT-L [3]	88.9M	1446	38.0	64.9
SCT-M	33.48M	162.9	36.8	61.2
SCT-L	59.89M	342.6	37.3	65.1